

Document downloaded from:

<http://hdl.handle.net/10251/182550>

This paper must be cited as:

Serrano, J.; García Martínez, A.; Monsalve-Serrano, J.; Martínez-Boggio, SD. (2021). High efficiency two stroke opposed piston engine for plug-in hybrid electric vehicle applications: evaluation under homologation and real driving conditions. *Applied Energy*. 282(Part A):1-17. <https://doi.org/10.1016/j.apenergy.2020.116078>



The final publication is available at

<https://doi.org/10.1016/j.apenergy.2020.116078>

Copyright Elsevier

Additional Information

# High efficiency two stroke opposed piston engine for plug-in hybrid electric vehicle applications: evaluation under homologation and real driving conditions

Applied Energy

Volume 282, Part A, 15 January 2021, 116078

<https://doi.org/10.1016/j.apenergy.2020.116078>

**José Ramón Serrano, Antonio García, Javier Monsalve-Serrano\* and Santiago Martínez-Boggio**

CMT - Motores Térmicos, Universitat Politècnica de València, Camino de Vera s/n,  
46022 Valencia, Spain

Corresponding author (\*):

Dr. Javier Monsalve-Serrano (jamonse1@mot.urpv.es)

Phone: +34 963876559

Fax: +34 963876559

## Abstract

The potential of plug-in hybrid electric vehicles (PHEV) to reduce greenhouse gas emissions highly depends on the vehicle usage and electricity source. In addition, the high costs of the battery pack and electric components suppose a challenge to the vehicle manufacturers. However, the internal combustion engine complexity can be reduced due to its lower use as compared to the no-hybrid vehicles. This work evaluates the use of a new opposed piston 2-stroke engine in a series PHEV architecture based on rod-less innovative kinematics along different driving routes in Europe. A OD-vehicle model fed with experimental tests is used. The battery size is optimized under homologation conditions for two different vehicle types. The optimum case is tested in several real driving conditions under different vehicle modes and battery states of charge. The main contribution of this work is the demonstration of the potential to reduce the vehicle CO<sub>2</sub> emissions and cost with an innovative 2-stroke engine. The results show that 24 kWh is the optimum battery size for both vehicle platforms. Charge depleting mode shows 70% of CO<sub>2</sub> tailpipe reduction in urban cycles and 22% in long travels compared to the no-hybrid version. Charge sustaining mode results show a CO<sub>2</sub> tailpipe reduction of 20% in urban cycles and 2% in long distance travels with respect to the no-hybrid version. In spite of the CO<sub>2</sub> contribution of the battery manufacturing, the results show a reduction of LCA CO<sub>2</sub> emissions in 52% in charge depleting and 7% charge sustaining against the no-hybrid case.

## Keywords

Plug-in Hybrid; 2-stroke engine; Opposed piston; Emissions regulations; Battery Package

## 1. Introduction

Future predictions of battery electric vehicles (BEV) market share vary from 18% to 57% of new vehicle sales in 2040. The level of fleet-wide hybridization is predicted to 60% in 2030 and 90% by 2040 [1]. This is a consequence of the strict European CO<sub>2</sub> targets for passenger cars and heavy-duty vehicles. Several authors affirm that it will be hard to homologate the fuel economy standards without a powertrain hybridization [2]. Several solutions have been studied in the last few years in terms of xHEV as mild-hybrid (MHEV, battery of <60V & <3 kWh), full hybrids (FHEV, battery of 300-600 V & 5-10 kWh) and plug-in hybrid (PHEV) with similar electric components as a battery electric vehicle (BEV, battery of 400-800 V & >20 kWh). The PHEV has similar powertrain layout than FHEV but with the possibility to re-charge the batteries with the external grid electricity [3]. In addition, the main difference with respect to a BEV is that the PHEV equips a range extender device, generally an internal combustion engine (ICE), that can extend the vehicle mileage to values even higher than a conventional no-hybrid vehicle. Generally speaking, all these solutions are expected to co-exist depending on the vehicle application in order to achieve the CO<sub>2</sub> target at fleet levels [4].

Automotive companies and researchers are currently exploring potential strategies for future development. Conway et al. [5] show that currently two ways are possible: 1) High-technology ICE with low levels of electrification or 2) High electrification combined with a simpler ICE version; the main justification is the trade-off existing in order to maintain a consistent development budget. Several authors reported CO<sub>2</sub> reductions between 10% to 20%, depending on the electrification level, using diesel ICEs with several powertrain architectures, with respect to the conventional no-hybrid vehicle [6][7]. However, the main limitation is the total vehicle cost due to the added equipment as the complex aftertreatment system (ATS) to achieve the Euro 6 levels and the electric components as the electric motor (EM) and battery pack. Therefore, this type of technology is restricted to expensive segment cars as class C sedan or sport utility vehicles (SUV). Gasoline engines were also studied in the past in hybrid powertrains with great success due to the reduction of the ICE operating time at low load (avoiding pumping and friction losses) and the possibility to use a three-way catalyst, less expensive than the diesel ATS [8][9]. Conway et al. [5] show that supplementing with 15 kW of electric assist provides equivalent gains than increasing 3 points in compression ratio (CR) for a 1.0 L engine and by nearly 1.3 CR points for a 2.0 L engine, assuming a baseline compression ratio of 10:1. Garcia et al. [10] studied a gasoline direct injection (GDI) spark ignited (SI) engine, variable compression ratio (VCR) in several powertrain architectures. The VCR system allowed fuel improvements of 3% in a conventional powertrain, 8% in MHEV and 17% in FHEV powertrains. The electrification level was found to be more determinant than the powertrain architecture (parallel, series or power split). The parallel was found to be the most effective to achieve low fuel consumption and emissions (NO<sub>x</sub> and Soot) in full hybrid applications. On the other hand, the main advantage of MHEV is the low cost and powertrain change with respect to current commercial vehicles. Therefore, MHEV is currently the most attractive option for vehicle manufacturers. Zanelli et al. [11] studied the effect of an electric supercharger in a 48 V system. The authors varied the turbine size, intake cam profile and compression ratio. The fuel economy could be improved by 5.1 g/km CO<sub>2</sub> over the worldwide harmonized light vehicles cycle (WLTC). However, it was found not

to be enough to achieve the 2025 European CO<sub>2</sub> targets (80 g/km) [12]. Lane et al. [4] show that PHEV solution allows to achieve zero urban tailpipe emissions with the same advantages of a FHEV in long distance trips. The main problems are the total vehicle cost due to large battery size as BEV and expensive ICE as an FHEV.

The second option appears as possible solution for the abovementioned powertrain. The decrease in the complexity and price of the ICE is currently a hot topic and several researchers and vehicle manufacturers are paying attention [13][14]. Plug-in hybrids with de-rated engines or small engines in order to maintain the battery charge when is depleted, is a possibility to strongly reduce the CO<sub>2</sub> emissions while maintaining reasonable vehicle costs [15]. This type of powertrain, also called range extender, has the properties of a pure electric vehicle but allows to continue travelling through the on-board fuel converter that converts a fuel, such as gasoline, into electrical energy whilst the vehicle is driving [16]. This solution overcomes the main problem of current BEVs due to long recharging times before the vehicle is available to be used. The large battery pack size and electric machine allows to achieve similar or higher brake power than a diesel or gasoline engine without tailpipe emissions. Several range extender concepts were studied as Wankel rotary engine [17], micro gas turbines [18], and small reciprocating piston engine [19]. Companies as MAHLE and Ricardo recently presented innovative gasoline engines for that purpose. In particular, MAHLE showed the potential of a two-cylinder and four-stroke port fuel injector (PFI) spark ignited engine with a maximum brake power of 30 kW and a brake thermal efficiency (BTE) of 37% dedicated to PHEV application [20]. This study identified that the efficiency was not given the highest priority due to the ICE is not the primary source of propulsive energy. Compared to other technologies the reciprocating piston engine offers the potential of low manufacturing cost, reasonable package size and a short development time. Fan et al. [21] show that the range extender engines can be predominantly operated at full load, thus the efficiency benefits of a diesel engine over a gasoline engine is reduced compared to a conventional application. In addition, it is possible to reduce the ATS cost. Therefore, range extender PHEVs with low complexity ICEs are a potential solution to reduce the CO<sub>2</sub> emissions in passenger vehicles.

In this work, a novel 2-stroke rodless opposed piston engine (2S-ROPE) high efficiency engine concept was studied as a mean of reducing the engine complexity and cost. The engine is mounted in a series PHEV powertrain. The two best-seller passenger vehicle platforms in Europe, class B-hatchback and a sport utility vehicle-SUV, are tested by numerical vehicle modelling. With this, the main contribution of the work is twofold. On one side, the analysis of an ultra-small engine in real driving conditions for the two best-selling passenger vehicle platforms in Europe. On the other side, the development of a methodology to select the right battery size for PHEV powertrains based on a OD vehicle numerical model with real driving data. The targets considered for the optimization process rely on minimizing the energy consumption and CO<sub>2</sub> emissions at tank-to-wheel (TTW), well-to-wheel (WTW) and life cycle analysis (LCA) levels. The real driving cycle database is generated in Spain and France to understand the effect of the electricity matrix on the total CO<sub>2</sub> reduction. Therefore, the contributions of the work can enhance the database for the development of new passenger vehicles to reduce the global air pollution together with lower vehicle design cost and time.

## 2. Methodology

### 2.1. Experimental engine test

The innovative spark ignition 2-stroke rod-less opposed piston engine was tested in an experimental test bench in order to characterize the fuel consumption and emissions. This engine has been patented, designed and manufactured by INNengine company [22] and loaned for the current work. It consists of a rotative mechanism based on a crank-shaft with faced cams perpendicular to the opposed piston skirts (Figure 1). Bearings located at the skirts of the opposed piston, rotate on the faced cams surface. The rotative movement of bearings at the opposed cylinders skirts generates tangential forces on the border of the face-to-face cams of the crank-shaft. These tangential forces applied at a distance of the crank-shaft center generate torque and lie for alternative-to-rotative movement conversion. Eight pistons are disposed in opposed pairs, sharing combustion chamber, as well as intake and exhaust ports.

This prototype already implements the variable ports-timing (VPT) and VCR systems, which enhance both efficiency and performance. It allows to make one power stroke per revolution, so it is also called one stroke engine. The main reasons of this approach, 2-stroke approach in combination with the two power strokes per turn and the 2 opposed piston per cylinder, is for mechanical losses reduction. They are achieved by means of avoiding the low-pressure loop (no pumping losses, but a scavenge pump is needed) and significant linear piston speed reduction (friction losses reduction).

The VCR is achieved by rotating the plates depicted in Figure 1 with a variation of 2.6 points in CR. The plates are also the components that transform the linear movement of the piston to the rotational movement of the output axle. Moreover, they allow to change the intake and exhaust open and close time. Table 1 summarize the main specifications of the engine. More details about the engine configuration can be seen in previous work of the research group [23].

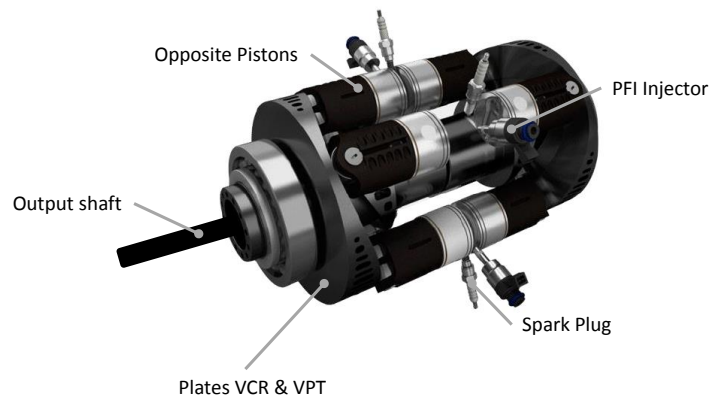


Figure 1 – 2S-ROPE INNengine schematic design and main components.

Table 1 - INNE engine specifications [23].

Engine Type	2 power strokes per engine revolution
Special configuration	Variable port timing (VPT) and variable compression ratio (VCR)
Fuel Injection	Port fuel injection
Number of cylinders	4 cylinders with opposed position
Air filling behaviour	Uniflow scavenging approach
Displaced volume	500 cm <sup>3</sup>
Weight	43 kg
Stroke	29.0 mm
Bore	52.4 mm
Compression ratio	9.5 to 12.1
Rated power @ 3500 rpm	33 kW (45 hp)
Rated torque@ 1000 rpm	123 Nm

The experimental campaign was performed in an engine test bench with measurements of in-cylinder pressure, intake and exhaust pressure and temperature among others (see Figure 2). The potential of this engine is based on its compactness, absence of vibrations and simplicity, going in hand with a very competitive figures in terms of power density and fuel consumption. The engine unit has been designed, assembled, and tested to analyze several performance aspects, such as gas exchange and combustion.

Engine performance as engine speed, brake torque, in-cylinder pressure, average intake and exhaust Pressure/Temperature and fuel consumption was measured. A Horiba Dynas 3 dynamometer and AVL 733S fuel balance are used. The experimental campaign is performed in 15 operative points. The engine speed and compression ratio were varied from 1000 rpm to 4000 rpm and 9.5:1 to 12.1:1, respectively.

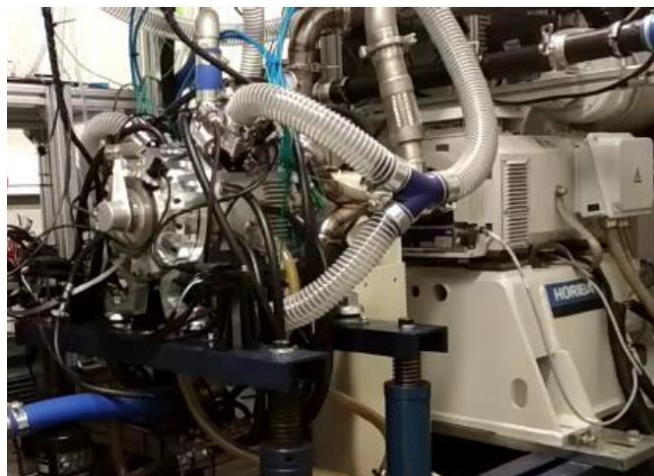


Figure 2 – Engine test bench with the 2S-ROPE fully instrumented for the experimental campaign.

Due to limited time available for testing the engine prototype, the data collected during the experiments were not enough to perform a complete engine map. However, a one-dimensional gas-dynamics engine model was developed and validated. The engine modelling activities have been performed with an in-house developed software called VEMOD, in which the special architecture and kinematics of 2S-ROPE has been programmed. More information about the experimental and modelling engine activities can be found in [23]. The model was used to predict 40 different operative conditions in terms of fuel consumption, CO<sub>2</sub> emissions and air-management and combustion process

parameters (air flow rate, scavenge efficiency, filling ratio, max cylinder pressure and temperature, exhaust gas temperature, CA50, CA10-90, etc). The engine speed was varied at 1000, 1500, 2000, 2500, 3000, 3500 and 4000 rpm. The VCR plate is varied to achieved CR of 9.6:1, 10.4:1, 11.1:1, 11.6:1, 11.9:1 and 12.1:1. Thus, the model output provided 42 operative conditions that were used to create the engine map of fuel consumption and brake power necessary for the vehicle modeling.

## 2.2. Range extender PHEV vehicle model

The range extender 2S-ROPE is inserted in a series PHEV powertrain as illustrated in Figure 3. The engine, front positioned in the vehicle, is coupled with the generator electric machine. The traction motor, which is connected to the wheel through the differential and axes, is in the back. This layout benefits the weight distribution and the regenerative braking recovery. As shown by Garcia et al. [24] the braking power needs to be distributed between the front and rear wheels to fulfill stability requirements. The ideal braking distribution ensures that front and rear wheels lock simultaneously. The mathematical expression of this curve was shown by Xu et al. [25] and depicts that in average the split is performed 65%/35% to rear and front, respectively. Therefore, more energy is recovered by using the traction motor in the rear wheels.

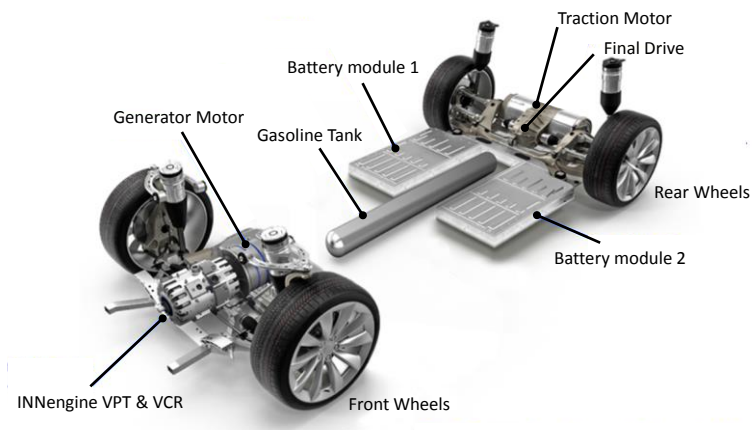


Figure 3 – PHEV range extender 2S-ROPE concept layout. Adapted from [26].



Two energy sources are used in this vehicle. One is the liquid fuel, in this case commercial gasoline, with the tank design along the central floor of the vehicle (Figure 3). The second source is the battery package, with one or two modules depending on the total energy of the pack. In this work, pouch A123 20 Ah and 3.3 V cells are used with arrangement in parallel and series connection. The voltage selected is 400 V to minimize the energy losses in the cabling and electric machines. In addition, this voltage allows to test the battery package from 8 kWh (121s – 1p) to 80 kWh (121s – 10p). The parametric study of the battery pack parallel cells allows to optimize the layout in order to achieve the minimum CO<sub>2</sub> emissions. More information about battery pack can be found in Appendix A.

The traction and generator motor are modelled by means of the efficiency maps against the rotational speed and torque. The Toyota Prius 2019 electric machine map is used as baseline and scaled by the method proposed by Petersheim et al. [27]. For this work, the generator is selected in order to regenerate the maximum power of the 2S-



ROPE. The traction motor is sized to achieve the same maximum brake power output than the commercial vehicle (propelled only by the ICE). Two vehicle platforms are evaluated, representative of the most sold passenger vehicles in Europe [28], a Hatchback and SUV. Table 2 shows the main specification of the no-hybrid vehicle in which the PHEV powertrain is inserted.

Table 2 – Vehicle no-hybrid main specifications [29].

Vehicle type [-]	HATCHBACK	SUV
Scheme [-]		
Base vehicle Mass [kg]	1155	1375
Passenger and Cargo Mass [kg]	100	100
Fuel [-]	Gasoline	Diesel
Fuel tank [l]	41	55
Vehicle Drag Coefficient [-]	0.29	0.31
Frontal Area [m <sup>2</sup> ]	2.20	2.38
Tires Size [mm/%/inch]	205/45/R17	215/65/R16
Gear ratio [-]	3.7/2.1/1.4/1.0/0.8	3.7/1.9/1.2/0.8/0.7/0.6
Differential ratio [-]	4.36	4.13
Engine [-]	1.0 SI	1.6 CI
Rated power [kW]	74	85
Top speed [km/h]	180	180
Acceleration 0-100 [s]	13.8	12.9

As a baseline, the two conventional powertrains are simulated at the same conditions of the PHEV range extender vehicle. To have a fair comparison, the engines used for the baseline (no-hybrid) are representative of the most technological current commercial gasoline and diesel ICE. The hatchback is equipped with a Ford EcoBoost 1.0 L gasoline GDI SI engine and the SUV with a Nissan 1.6 L turbo diesel Euro 6-d temp engine. Both engines were studied in the past by the research group and the engine maps can be found in [10] and [7], respectively. The brake specific maps are illustrated in Appendix B. Therefore, this work makes a comparison between the most advanced commercial engine against the proposed 2S-ROPE PHEV prototype.

### 2.3. Homologation and real driving cycle evaluation

Several authors [30,31] have demonstrated the importance of the driving cycles in the final vehicle fuel consumption and emissions. In the case of PHEV, the country of study and the battery re-charge times in a day are important parameters due to the use of the electricity grid as an energy source. Therefore, to have a global overview of the potential of the proposed technology, homologation conditions in Europe and real driving cycles in different countries are considered.

The worldwide harmonized light-duty vehicles test procedure (WLTP) set the homologation rules that apply to all the new passenger cars across the EU since September 2017. This procedure includes electric vehicles and all types of hybrid



vehicles. In particular, for PHEV the normative sets several special conditions to have a fair comparison against the other vehicle types. PHEVs operate under two modes called: charge depleting (CD) and charge sustaining (CS). Extra modes as battery charging and sport are used by the manufacturers. However, as it is not contemplated by the WLTP, there are not included in the current work. Charge depleting and charge sustaining modes are illustrate in Figure 4 for a vehicle tested under 3 consecutives WLTC. As the pure electric range changes depending on the battery total energy and the initial state of charge (SOC), the WLTP establishes that in CD the vehicle needs to perform the necessary WLTP cycles up to the battery is totally depleted (SOC=0.35). In homologation conditions, the vehicle starts with the battery totally charged (SOC=1.0). Immediately after testing, the vehicle is reconnected to a charger. The energy necessary to re-charge the battery is measured and added in the final vehicle homologation. The CS always represents one WLTC with the battery charge oscillating around 4% of the necessary energy to complete the driving cycle. The parametric implementation of the limits for the SOC in charge sustaining mode is due to the large difference of energy that PHEV carry in their batteries. This ensures a fair comparison between vehicles.

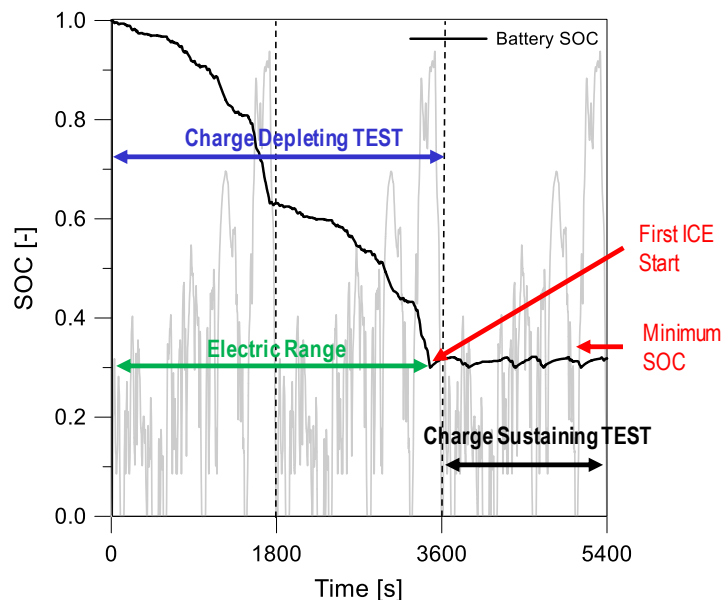


Figure 4 – Homologation cycle under the new WLTP legislation for light duty vehicles.

For the final emissions and fuel energy consumption, the WLTP uses the utility factor (UF) defined in the SAE J2841. The UF represents the proportion of vehicle distance traveled electrically. Therefore, the UF increases with their electrical range for a PHEV. In this work, the UF is calculated for each vehicle configuration and the final results for the homologation case are depicted with this compensation.

In terms of real driving cycles, Spain and France are studied by the use of GT-RealDrive tool. This feature allows fast and remote generate driving cycles in different countries around the world with real traffic data and signals. The necessary inputs are the initial and final destination. The countries selection is done for two representative scenarios in Europe with different electricity mix CO<sub>2</sub> contribution. More details are added in the life cycle analysis section. To evaluate different conditions, the capital city of both countries (Madrid and Paris, respectively) is considered with 10 urban cycles, 10 urban-rural and 10 city-city cycles. These cycles are taken aleatory with the urban cycles

all inside the city, the urban-rural performed from the city center to neighbor town and the city-city cycles performed from the capital city to the main cities around the country. Examples of two urban cycles performed with GT-RealDrive can be seen in Figure 5. The main statistical parameters for the driving cycles are shown in Table 3. The 60 routes sum 9881 km and 134 hours of travel. This is the main advantage of powertrain simulation due to the possibility to reduce the vehicle development cost and time. In addition, the use of the GT-Real Drive allows to quickly generate the vehicles routes from a remote position and fast. The speed against time profiles for all the cycles is illustrated in Appendix B.

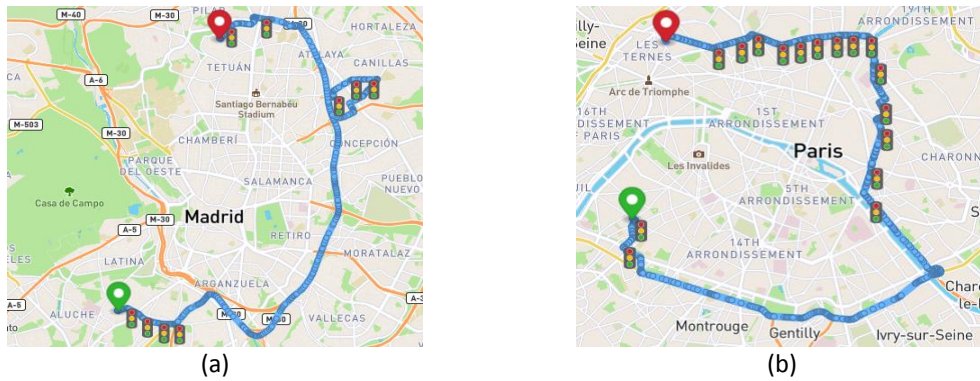


Figure 5 – Urban cycles in Madrid (a) and Paris (b).

Table 3 – Mains average statistical parameter for the different real driving routes in Spain and France.

Country	Route Type	Number of routes	Total Distance [km]	Average Distance [km]	Average Time [min]	Average Speed [km/h]	Vapos95 [m <sup>2</sup> /s <sup>3</sup> ]
Spain	Urban	10	148	14.8	35.9	20.0	23.0
	Urban-Rural	10	380	38.0	46.3	41.0	26.9
	City-City	10	4545	454.5	324.9	78.5	28.6
France	Urban	10	151	15.1	45.0	15.5	19.3
	Urban-Rural	10	492	49.2	58.4	41.0	28.0
	City-City	10	4165	416.5	296.0	77.2	27.1

As was mentioned before, many factors impact the vehicle fuel economy. This work is focused on factors that are specific to PHEV and directly related to the vehicle usage. We discard factors such as driver aggressiveness or the use of auxiliaries since these are also relevant for conventional vehicles. Instead, our emphasis is on driving patterns taken from mobility data in several conditions that the PHEV 2S-ROPE can be used to understand the potential of the proposed technology against current market technologies. Two possible PHEV modes (Electric CD and Hybrid CS) and three different state of the charge from fully depleted to totally charged are tested (0.35, 0.60 and 1.0). The matrix of the test modes is shown in Table 4. The different cases are studied in the 60 cycles and in the WLTC under the same conditions.

Table 4 – PHEV modes and Initial state of the charge tested for the homologation and real driving cycles.

Initial SOC	Electric CD	Hybrid CS
Maximum SOC (1.0)	X	
Medium SOC (0.60)	X	X
Min SOC (0.35)		X

## 2.4. Life cycle analysis model

The potential of plug-in hybrid electric vehicles to reduce greenhouse gas emissions highly depends on the vehicle usage and electricity source. The European targets in tank-to-wheel planned for 2021 up to 2030 are shown in Table 5. However, the real potential of a new technology needs to be considered with well-to-wheel and life cycle analysis assessment. The European community estimates that well-to-wheel targets will be added to the normative by 2030 [32].

Table 5 – European tank to wheel (TTW) CO<sub>2</sub> fleet average targets for the next years [33].

Parameter	Limit [g/km]
CO <sub>2</sub> 2021 Target	95
CO <sub>2</sub> 2025 Target	80
CO <sub>2</sub> 2030 Target	67
CO <sub>2</sub> Taxes incentive	50

In this work, the three parameters (TTW, WTW and LCA) are considered and analyzed for the homologation and real driving cycles. For the WTW, this means to include the well-to-tank CO<sub>2</sub> emissions ( $WTT_{CO_2}$ ) by the energy consumption depending on the source (liquid fuel or electricity) and sum with the estimated tailpipe CO<sub>2</sub> emissions ( $TTW_{CO_2}$ ) by the vehicle model approach. Equations 1 to 3 shows the required parameters for the analysis.

$$WTT_{CO_2} \left[ \frac{g_{CO_2}}{km} \right] = CO_{2\text{Fuel production}} \left[ \frac{g_{CO_2}}{kWh_{fuel}} \right] * Energy_{\text{Fuel consumption}} \left[ \frac{kWh_{fuel}}{km} \right] \quad (1)$$

$$TTW_{CO_2} \left[ \frac{g_{CO_2}}{km} \right] = CO_{2\text{Fuel consumption}} \left[ \frac{g_{CO_2}}{km} \right] \quad (2)$$

$$WTW_{CO_2} \left[ \frac{g_{CO_2}}{km} \right] = WTT_{CO_2} \left[ \frac{g_{CO_2}}{km} \right] + TTW_{CO_2} \left[ \frac{g_{CO_2}}{km} \right] \quad (3)$$

The  $CO_{2\text{Fuel production}}$  is shown in Table 6, the  $Energy_{\text{Fuel consumption}}$  is calculated with the vehicle numerical model along the driving cycle as well as the  $CO_{2\text{Fuel consumption}}$ .

The carbon intensity of the European electricity mix ( $CO_{2\text{Fuel production}}$  by the electricity source) was taken from the International Energy Agency for all the countries. **¡Error! No se encuentra el origen de la referencia.** shows the average grams of CO<sub>2</sub> emissions per kWh in 2019 by country taken from the report [34]. These results consider the electricity traded between countries, affecting the carbon intensity of the electricity consumed at national level. The selected case of study, Spain and France, was taken since it proposes representative conditions of the average EU electricity mix and an ultra-low CO<sub>2</sub> production country, respectively. In addition, as shown in **¡Error! No se encuentra el origen de la referencia.**, both countries are in the top five of the countries that produces the highest CO<sub>2</sub> emissions in Europe.

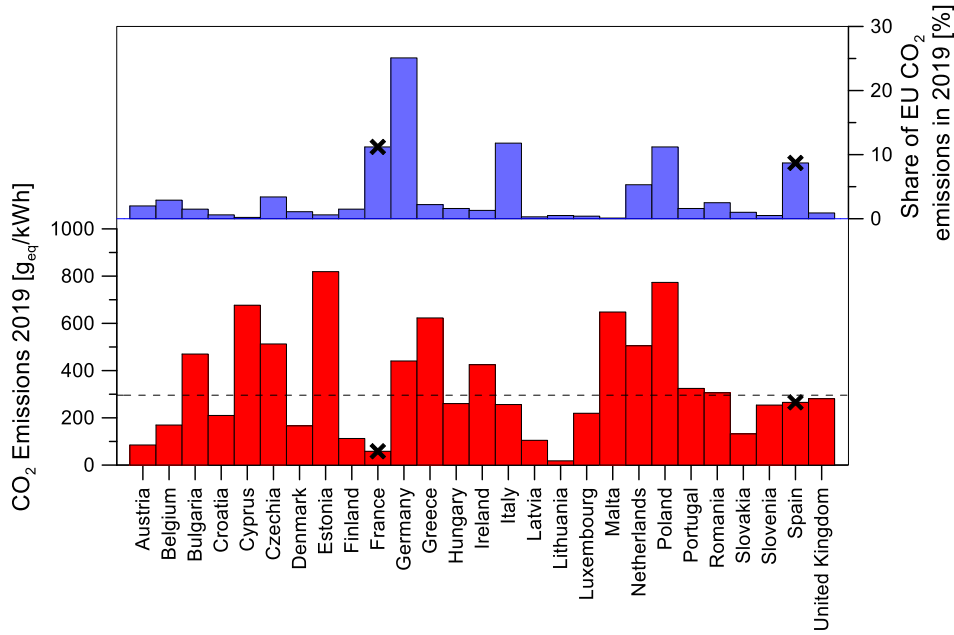


Figure 6 – CO<sub>2</sub> electricity mix emissions (a) and CO<sub>2</sub> share (b) by country in the European communion. Data obtained from [34].

Later, the LCA is calculated. This parameter generally considers all the vehicle manufacturing, materials, maintenance and end of life (disposal and recycling). However, only the battery manufacturing is considered in this work. The main reason of this hypothesis is the similarities of the vehicles in no-hybrid and plug-in hybrid layout (structure and main components) and the lack of information about the special components, as the different ICE or EM, in terms of  $LCA_{CO_2}$  emissions impact. Qiao et al. [35] demonstrates that the battery manufacturing and disposal are the main parameters in an LCA comparison between electric, hybrids and other vehicle platforms. Equation 4 shows the LCA calculation.

$$LCA_{CO_2} \left[ \frac{g_{CO_2}}{km} \right] = WTW_{CO_2} \left[ \frac{g_{CO_2}}{km} \right] + CO_{2\text{Battery production}} \left[ \frac{g_{CO_2}}{kWh_{\text{battery size}}} \right] \quad (4)$$

$$* \text{Battery total energy} [kWh_{\text{battery size}}] * \frac{1}{\text{Vehicle life} \left[ \frac{1}{km} \right]}$$

The  $CO_{2\text{Battery production}}$  is show in Table 6. The information is taken from a technical review of the International Council on Clean Transportation (ICCT) [36] with more than 10 references of different works along the last few years. The average, maximum and minimum values are taken from the review to study the different scenarios. Battery manufacturing and disposal-recycling are considered by [36]. It is important to note that for the LCA is necessary to predict the vehicle use life (*Vehicle life*). The work by Dun et al. [37] is used to predict the use of a gasoline and diesel vehicle. The mentioned work estimates 160,000 km and 208,000 km, respectively. It is supposed that in this range, the battery is not necessary to be replaced for the gasoline version. However, due to the extend range and possible battery calendar aging, it is taken one replace for the SUV. This assumption is in line with the prediction of Toyota about their battery life [38]. In this work, it is assumed that the vehicle performance is maintained during the years due to the battery replacements consideration.

Table 6 - Main process evaluated in the LCA model.

Section	Country	Energy Source	CO <sub>2</sub> production [g/kWh]	Reference [-]
Well-to-Tank (WTT)	-	Commercial Gasoline	77.4	[39]
		Commercial Diesel	60.4	
Battery Production (LCA)	Spain	Electricity mix	265.8	[34]
	France		58.5	
	-	Maximum	344,000	[36]
	Average	139,773		
	Minimum	40,000		

### 3. Results and discussion

The results section is organized as follows: First, a performance analysis is carried out. The calibration engine maps obtained from the experimental investigation and 1-D engine model are presented. The maximum brake power is used to evaluate the two vehicle platforms performance against several road grade and vehicle speed. This is a key point to understand the differences between a plug-in series hybrid, equipped with the 2S-ROPE, against the commercial vehicle. Second, the battery size of the PHEV is optimized under WLTP conditions. Minimum energy consumption and minimum environmental effect are set as targets. Lastly, the optimum cases are tested under 480 different driving conditions including different real driving cycles (sixty cycles), initial battery state of charge (four different SOC<sub>ini</sub>) and PHEV operative mode (CD and CS modes).

#### 3.1. Performance

The obtained brake power output and brake specific fuel consumption is presented in Figure 7. The maximum brake power, 32 kW, was found at 3600 rpm and CR of 11.5:1, as shown Figure 7 **Error! No se encuentra el origen de la referencia.a**. In terms of fuel economy (see Figure 7 **Error! No se encuentra el origen de la referencia.b**), the same region was found as the most efficiency with a minimum brake specific fuel consumption (BSFC) of 240 g/kWh (BTE of 35.6%). In general, for range extender applications, two to three operative conditions with different brake power are selected to fulfill different driving situations. In this engine, 32 kW (3600 rpm and 11.5:1 CR) and 20 kW (3000 rpm 10.4:1 CR) are selected to be used as charging point for the PHEV. The similar engine speed of the two different points reduces the transient phases and enhances the results in terms of engine noise, vibration, and harshness (NHV) and fuel consumption. These

engine maps are used to later feed the 0D vehicle numerical model in order to study the PHEV range extender 2S-ROPE behavior and potential CO<sub>2</sub> gains.

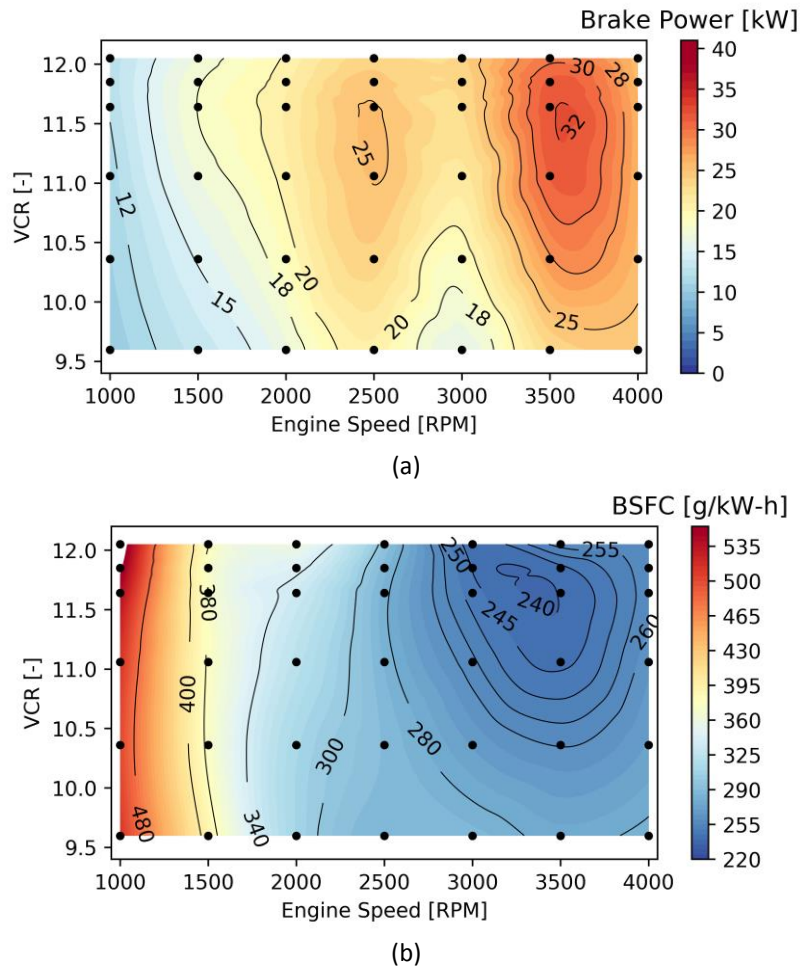


Figure 7 – Engine calibration map estimated by the 1D gas-dynamic engine model validated with experimental results. Brake power (a) and brake specific fuel consumption (b) against engine rotational speed and compression ratio.

The experimental campaign shows that the engine combines suitable qualities for small range extender vehicle applications as the small size and light weight with ultra-low vibrations and noise. In addition, the design combines properties of pure two-stroke engines (compact, powerful, and simple) with qualities of four-stroke engines as efficiency and the layout of opposed piston engines that benefits the fuel consumption and emissions. The highest brake thermal efficiency is at the level of complex SI gasoline engines with the abovementioned advantages for range extender applications.

The hatchback and SUV are analyzed under different driving speed, road grade and cargo mass. The analysis is performed by the calculation of the wheel forces from the ICE torque curve and multiplying by the transmission gear ratios (five gears for the hatchback and six gears for the SUV) and the final drive ratio for the no-hybrid case. On the other hand, for the PHEV is necessary to take the traction motor torque curve and multiply only by the final drive ratio. The hybrid case includes the charge depleting and charge sustaining modes. The last mode considers the maximum continues wheel force that can be provided without discharging the battery. This means the ICE-electric generator power plus the electrical losses. The vehicle wheels torque is compared against different road grades ranging from 0% to 45% (see Figure 8).

Figure 8a shows the wheel forces for the no-hybrid version and the plug-in hybrid version for the hatchback case. Since the traction motor is selected to obtain the same maximum power than the conventional vehicle, the curves for the no-hybrid version achieve the same power than the PHEV at maximum speed before the gear change. Therefore, the PHEV has higher wheels force at the same vehicle speed for all the gears except the first gear. This behavior is caused by the high reduction that allows the transmission at low vehicle speed. However, at ultra-low vehicle speed (below 20 km/h) the hybrid has better performance. The charge sustaining mode is a critical mode in the design of a plug-in hybrid powertrain. The 2S-ROPE 32 kW max power ICE allows to achieve 140 km/h in a flat road and 110 km/h with 5% of road grade when the battery is totally depleted. Figure 8b shows similar trend but for the SUV PHEV 85 kW traction motor case and the no-hybrid diesel version.

It is important to note that Figure 8 is performed in WLTP conditions, with one passenger and the fuel tank fully loaded. Other conditions are shown in Appendix D. In charge sustaining mode with four passengers and 5% road grade, the PHEV hatchback can achieve 100 km/h and the SUV 90 km/h (Figure D1). The behavior under these conditions is acceptable and can be affirmed that the vehicle has similar performance at high vehicle speed (>60 km/h) and PHEV even better at low vehicle speed (<60 km/h). One problem for the SUV can be the use of a trailer (1000 kg extra) in charge sustaining mode. Figure D2 shows that the vehicle can only achieve 70 km/h with 5% of road grade. A future improvement can be increasing the 2S-ROPE maximum brake power. However, for the conditions tested in this work the proposed ICE size is acceptable.

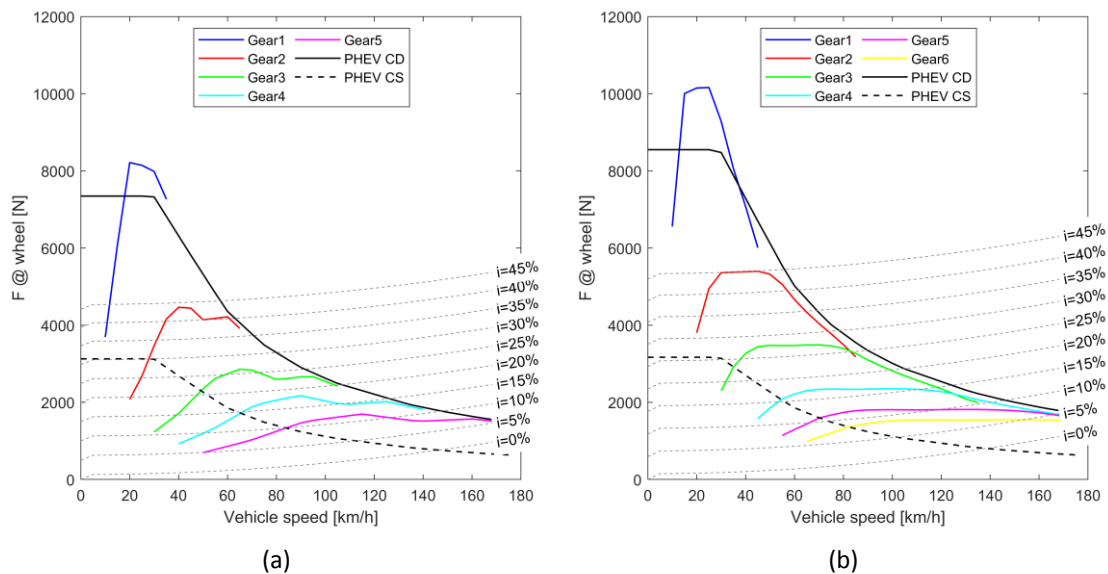


Figure 8 – Performance curves for PHEV and no-hybrid vehicles in homologation conditions in platform hatchback (a) and SUV (b).

### 3.2. Optimization under homologation conditions

The use of an ICE as range extender avoids the users concerns about the vehicle range as in the case of BEVs. However, Graham-Rowe et al. [40] found that users wanted to maximize the distance covered using electricity alone. Doing short trips on pure electric mode is one of the most important factors to buy a PHEV. Therefore, the analysis of the electric range mode appears as key point in this type of hybrid vehicles. To



perform this study, the WLTP normative is followed by running the vehicle under several consecutive WLTC after the battery is totally depleted. Figure 9a shows the electric range for different battery sizes. The number of parallel cells is increased from one (8 kWh) to ten (80 kWh) maintaining 400 V as nominal voltage (121 series cells). The hatchback, due to the lower vehicle weight and aerodynamic resistance, achieves 7 km more at the lowest battery size and 43 km more at the maximum case than the SUV. With 40 kWh (medium battery size of the selected range) it can be performed 7.5 and 6.4 consecutive WLTC for the hatchback and SUV, respectively. The utility factor is calculated to compensate the measurement consumptions as indicates the WLTP. Beyond 40 kWh, the variation of the UF is minimum.

The fuel consumption results (liquid fuel in the ICE, Figure 9b) shows that the PHEV version can achieve a combined CD+CS below 2.0 l/100km and 3.0 l/100km for the hatchback and SUV, respectively. These values are strongly reduced from the 5.4 lt/100km and 4.7 lt/100 km of the no-hybrid versions. In spite of the higher vehicle weight and aerodynamic resistance of the SUV, the higher density of diesel than gasoline allows to achieve lower volume consumption in the no-hybrid cases. When the battery is totally depleted, the charge sustaining PHEV mode is used. As the battery charge needs to be maintained, the ICE is turned on several times. The fuel consumption increases and the results are close to the no-hybrid cases. For the hatchback, the PHEV fuel consumption is lower than the no-hybrid case below 60 kWh. After this point, the battery weight has higher influence than the gain for lower energy losses in the battery package. The SUV, due to the use of gasoline in the PHEV instead of diesel as the no-hybrid, increases the fuel consumption around 1.0 lt/100 km.

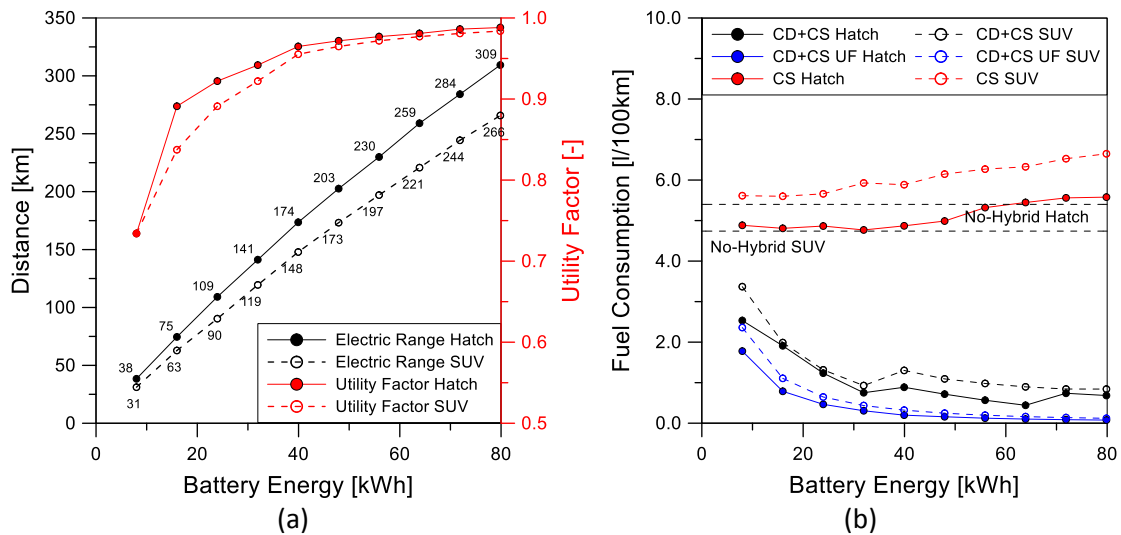


Figure 9 – Electric Range (a) and volume fuel consumption (b) under WLTP conditions for the hatchback and SUV.

Figure 10a shows the energy consumption for the different platforms considering the density of the fuels and the energy of the electricity grid needed to recharge the batteries from totally depleted to fully charged. For the PHEVs, the two energy sources (fuel + electricity) and its sum are shown for comparison against the baseline case. As it can be seen, the total energy decreases up to a certain battery size after which it remains flat. For the hatchback is 40 kWh and the SUV 48 kWh. This trend is caused by the balance between the improvement to use only the electric machine fed

by the battery as power source and the increase of the vehicle weight. The first improves the global vehicle efficiency due to the high efficiency of the traction motor with respect to the ICE-generator conversion. On the other hand, for light-duty vehicles, the impact of the addition of more parallel cells is strong. As one of the main targets is the minimum energy consumption, the two minimum cases are used in the real driving cycles analysis as optimum cases. For these two cases, the WLTC in charge sustaining mode shows lower energy consumption than the no-hybrid for the hatchback. However, the SUV shows a slight increase due to the high efficiency provided by the diesel engine. Therefore, in homologation condition, the SUV with the 2S-ROPE allows to reduce the ICE complexity but it is less efficient if the battery is not frequently charged (after 148 km, see Figure 9a).

The quantification of the environmental impact is the other main objective of this study. Figure 10b shows the tank-to-wheel CO<sub>2</sub> emissions produced. This means the CO<sub>2</sub> produced by the engine when is used. Both PHEV platforms are below 50 g/km (CO<sub>2</sub> taxes incentive) and far below 2025 and 2030 targets (see Table 5). On the other hand, as seen in the energy consumption, the only use of charge sustaining is a problematic mode for the PHEV with values 12 g/km below the no-hybrid version for the hatchback and 10 g/km higher than the diesel no-hybrid for the SUV.

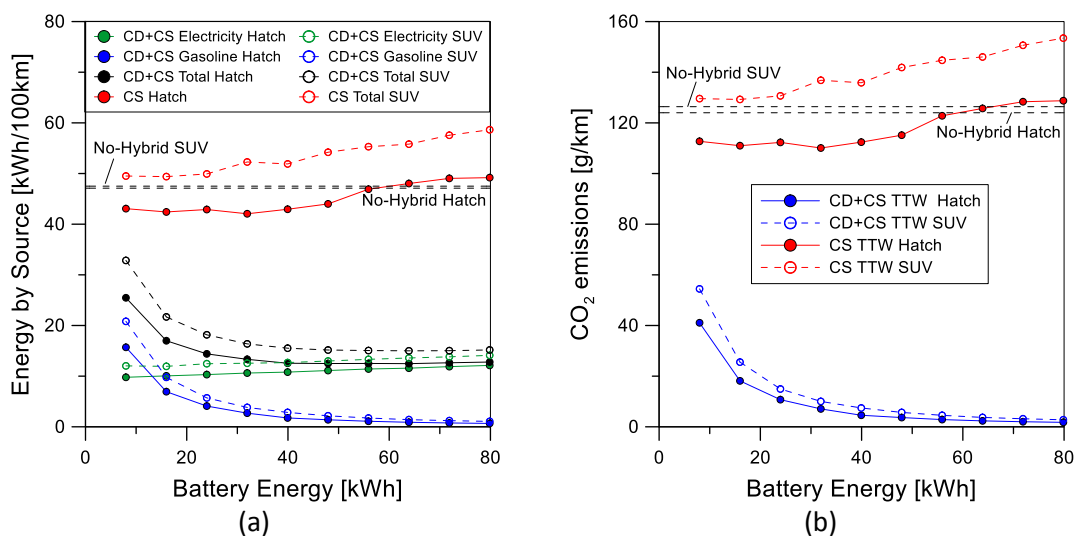


Figure 10 – Energy consumption by source (Liquid Fuel, Electricity and the total energy consumed) (a) and tank-to-wheel (TTW) CO<sub>2</sub> emissions (b) for the hatchback and SUV under WLTP conditions.

As several energy sources are used, it is necessary to consider the impact of the CO<sub>2</sub> in a well-to-wheel basis. The electricity mix of Spain and France is added to the previously shown TTW results in Figure 11. The total WTW CO<sub>2</sub> emissions shows the strong impact in PHEV of the electricity path. For CD+CS with the French mix is possible to reduce by 92% and 89% the CO<sub>2</sub> emissions of the hatchback and SUV as compared to the no-hybrid case, respectively. In the case of Spain, the benefits are 78% and 72% for the mentioned vehicles with respect to the no-hybrid version. It is important to note that the CS maintains the same values of the TTW due to the same initial and final battery state of the charge.

These results are complemented with the life cycle analysis shown in Figure 12. As was mentioned, the battery manufacturer and disposal were the unique factors added. In this sense, three scenarios regarding the CO<sub>2</sub> production relative to the battery

production are considered (see Table 6). As shown in Figure 12 for both vehicles, the increase of the battery size has a negative effect. The minimum battery size found for the best vehicle efficiency is 24 kWh for both platforms. The balance between higher vehicle efficiency and LCA CO<sub>2</sub> emissions reduces the size of the battery selected. A summary of the results is presented in Table 7. These two optimums are added to the previous optimum cases in the analysis under real driving conditions and PHEV modes in the next section.

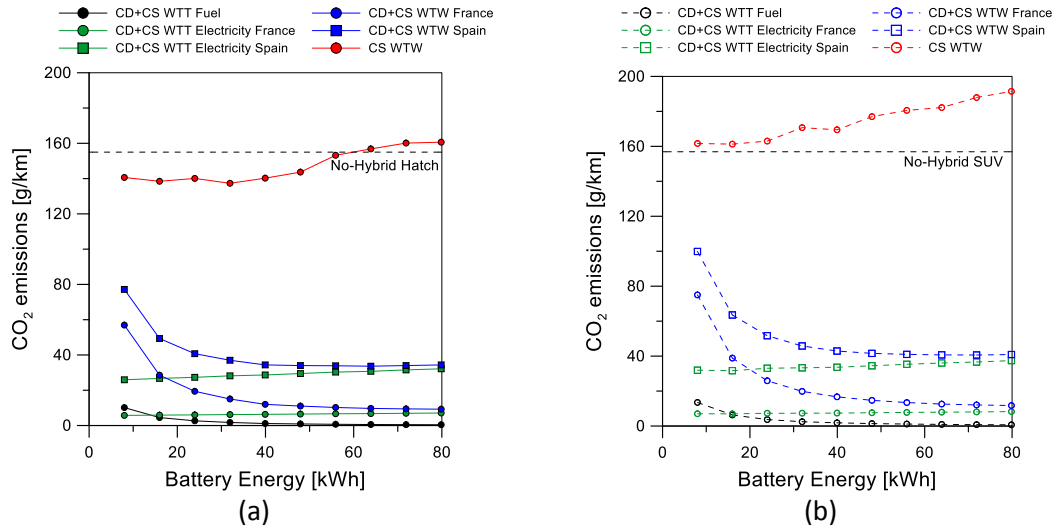


Figure 11 – Well-to-wheel (WTW) CO<sub>2</sub> emissions for the hatchback (a) and SUV (b) under WLTP conditions.

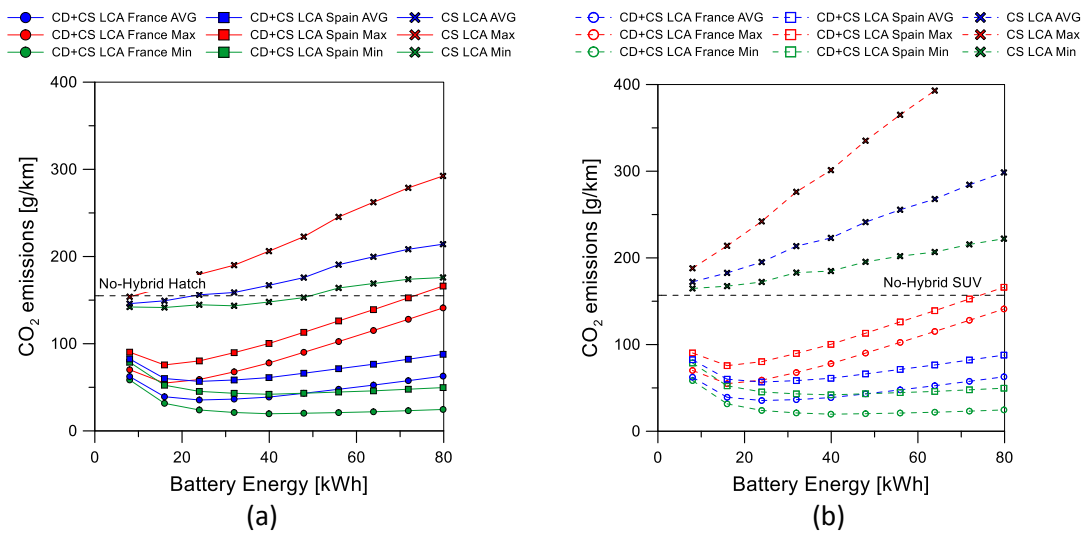


Figure 12 –Life cycle analysis (LCA) CO<sub>2</sub> emissions for the hatchback (a) and SUV (b) under WLTP conditions and three battery carbon intensity values.

Table 7 - Optimum selection under WLTP conditions

Vehicle Platform	Case	Battery Energy [kWh]	Electric Range [km]	Fuel consump CD+CS [l/100km]	Fuel consump CS [l/100km]	Total Energy consump [kWh/100km]	LCA Spain CO <sub>2</sub> [g/km]	LCA France CO <sub>2</sub> [g/km]
Hatch	Baseline	-	-	5.4		47.5	155	
	Opt Energy	40	174	0.20	4.8	12.7	62	38
	Opt CO <sub>2</sub>	24	109	0.47	4.9	14.5	57	35
SUV	Baseline	-	-	4.7		47.1	157	
	Opt Energy	48	148	0.25	6.1	15.2	66	44
	Opt CO <sub>2</sub>	24	90	0.65	5.9	18.2	57	35

### 3.3. Real driving cycles evaluation

In this section, two countries and three type of driving cycles are used. GT Real Drive tool allows to generate different routes around the world including the real traffic data as congestion level and signals. Three initial SOC levels are tested in the two PHEV modes. The CD+CS case represents the battery fully charge (CD+CS 1.0) or 60% charged (CD+CS 0.6), running under electric mode up to the battery is totally depleted. The vehicle continues in range extender mode also called CS. Therefore, the cycle is named as the composition of both phases. If the cycle is short enough, the vehicle can only run under EV mode. Lastly, CS mode represents the vehicle with the battery 60% charged (CS 0.6) or completely discharged (CS 0.35) running as a full hybrid or charge sustaining vehicle mode. At the start and end the battery has the same energy storage. The section is organized by analyzing the hatchback vehicle with the battery size corresponding to the optimum of energy consumption (40 kWh). Later, the other optimum and the SUV cases are summarized in final table for the brevity of the manuscript.

Figure 13 shows the results for the urban cycles in Spain and France created from a location inside the city of Madrid and Paris, respectively. The total energy consumption by 100 km is shown for each cycle and the average of the ten cycles is represented with a dashed line. The SOC 0.6 allows better results due to the lower internal resistance of the battery in the range of SOC 0.8 to 0.4. Similar results are seen in France (Figure 13b), with higher decrease with respect to the no-hybrid gasoline version due to a slightly increase of the baseline. This is caused by the higher congestion levels of Paris (lower average distance and higher travel time than Spain, see Table 3). The PHEV version is not affected by this condition and maintains the energy consumption of Spain.

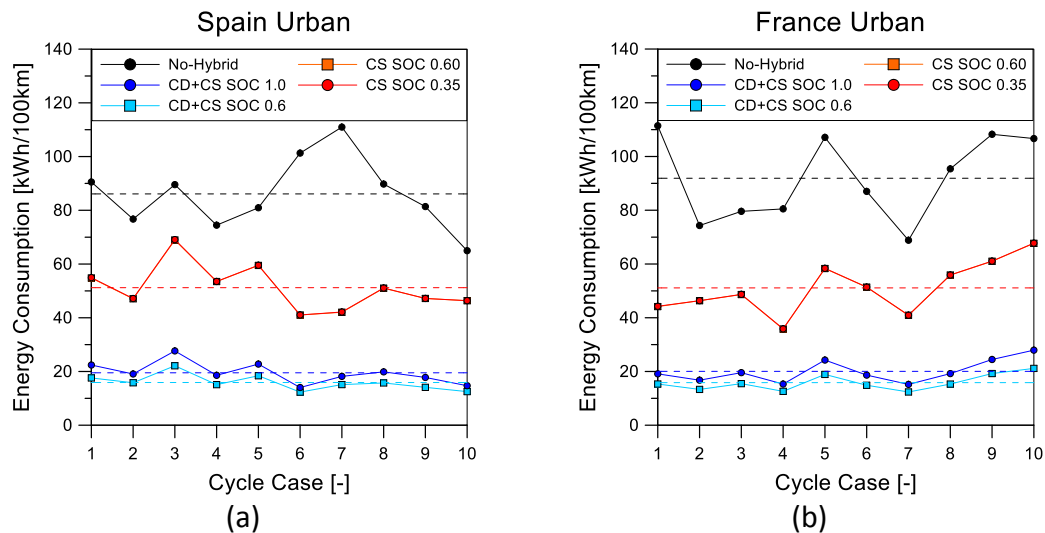


Figure 13 – Urban energy consumption by cycle and average values in Spain (a) and France (b) for the hatchback with battery selection for minimum energy consumption (40 kWh). Average of the 10 cycles for each case is presented in dashed line with the same color of the corresponding case.

The urban-rural (created from the city center to a neighbor town) and city-city cycles (from the city center to other city center of a principal city of the country) results for the hatchback with 40 kWh of battery package are shown in Figure 14 and Figure 15, respectively. In charge depleting mode, the improvements in average for the urban-rural cycle continue being extremely good with 70% of reduction in both countries (see Figure 14). The charge sustaining mode shows a reduction with respect to the urban results due to higher highway phases (22 km/h higher average speed than the urban cycles). The average energy consumption reduction is 23% for the proposed vehicle powertrain with respect to the baseline. It is important to note that in electric mode (mostly CD) the vehicle energy consumption is similar for all the cycles and not suffers the variations found in CS mode and no-hybrid version (see Figure 13 and Figure 14). This is caused by the high efficiency of the electric machine (>80%) with respect to both ICE version proposed (<35%) for the hatchback vehicle. This allows to make the consumption flat in all driving conditions. This is an interesting result from the perspective of the low influence of the urban conditions in the final results. Totally different from a no-hybrid vehicle study.

The city-city cycles, with more than 400 km each route, suppose hard conditions for the proposed PHEV 2S-ROPE vehicle. However, the results depicted in Figure 15 are favorable for the PHEV version with a 32% improvement in CD and the battery totally charged with respect to the no-hybrid. The large battery package equipped in this optimum allows a larger pure electric mode driving. This is also seen in the increase of energy consumption when the travel is started with 60% of the charge. The reduction decays up to 15%. Lastly, the charge depleting mode in both states of the charge allows 4% of energy consumption reduction. The higher brake thermal efficiency of the ICE (comparison between one single point in the 2S-ROPE and the average value for the DISI gasoline engine) and the energy recovery in the initial and final urban phases allows to this mode to be more efficient than the no-hybrid. The Spain and Paris city-city cycles do not show great differences, with only slightly higher energy consumption in the case of the cycles in Spain due to higher average vehicle speed and accelerations (see average speed and Vapos95 in Table 3).

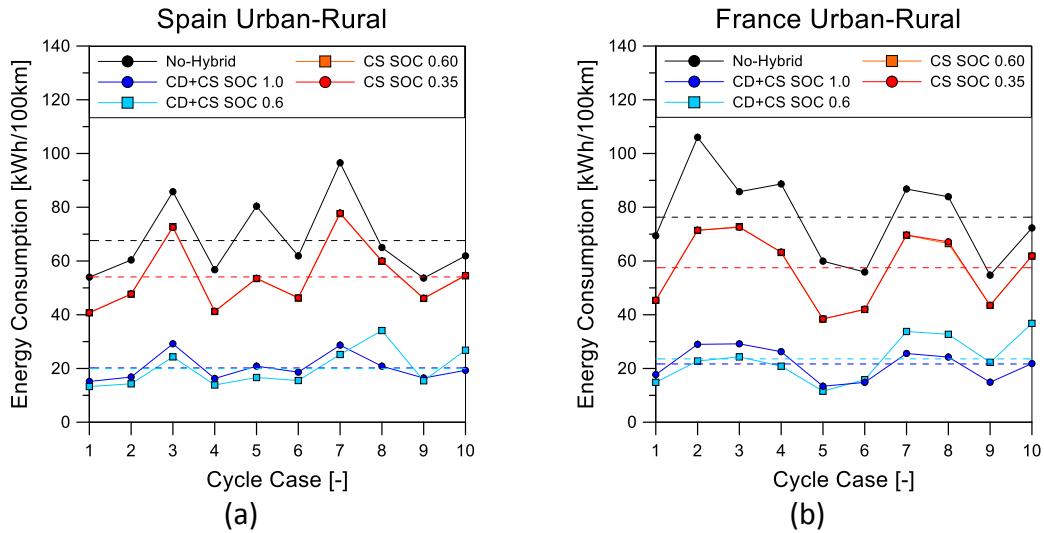


Figure 14 – Urban-Rural energy consumption by cycle and average values in Spain (a) and France (b) for the hatchback with battery selection for minimum energy consumption (40 kWh). Average of the 10 cycles for each case is presented in dashed line with the same color of the corresponding case.

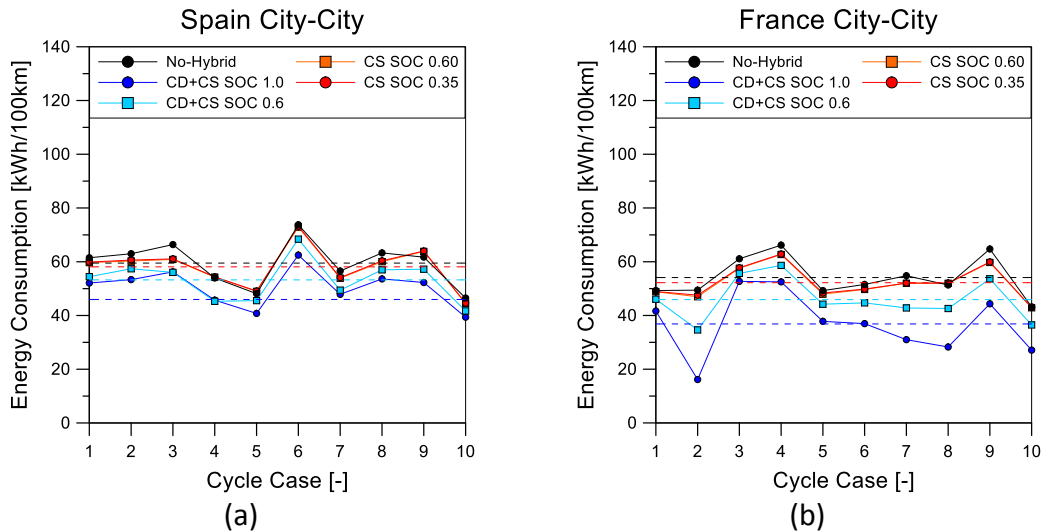


Figure 15 – City-to-City energy consumption by cycle and average values in Spain (a) and France (b) for the hatchback with battery selection for minimum energy consumption (40 kWh). Average of the 10 cycles for each case is presented in dashed line with the same color of the corresponding case.

The energy consumption is one of the main targets in the development of a new vehicle powertrain. However, in the last few years the greenhouse gasses emissions and their impact in the global warming appears a new key issue. Therefore, the CO<sub>2</sub> emissions at different analysis levels are included for the real driving cycles. Figure 16 shows the TTW, WTW and LCA CO<sub>2</sub> emissions for the different cases of study in the no-hybrid and PHEV 2S-ROPE hatchback vehicle. The average total emissions (AVG LCA) for each vehicle mode and country is also added. Figure 16a shows the results for the no-hybrid and PHEV 40 kWh (optimum in energy reduction for homologation conditions). The results show a strong improvement of the CO<sub>2</sub> emissions with 217 g/km for the no-hybrid, 95 g/km in CD mode and 196 g/km CS mode. In spite of the current European targets do not contemplate the values at this level (only TTW), the CO<sub>2</sub> emissions reduction are notable even considering the effect of the battery pollution during the

manufacturing, with reductions between 10% and 55% depending on the battery re-charging frequency. In addition, Figure 16a shows that in urban and urban-rural cycles always ran as pure electric (zero TTW values) when the battery is totally charged. For the battery being at 60% of capacity, the urban-rural needs short periods of the engine on.

To have a comparison against other battery sizes, Figure 16b shows the percentage difference between the values found with 24 kWh and 40 kWh. The results in terms of LCA CO<sub>2</sub> emissions are favorable for the lower battery size except for some cases of urban-rural and city-city. The main reasons are the double effect of extra weight and high impact of the CO<sub>2</sub> in the battery production. In addition, for analysis in which only one cycle consecutive cycle is considered, the large battery size does not have significant benefits.

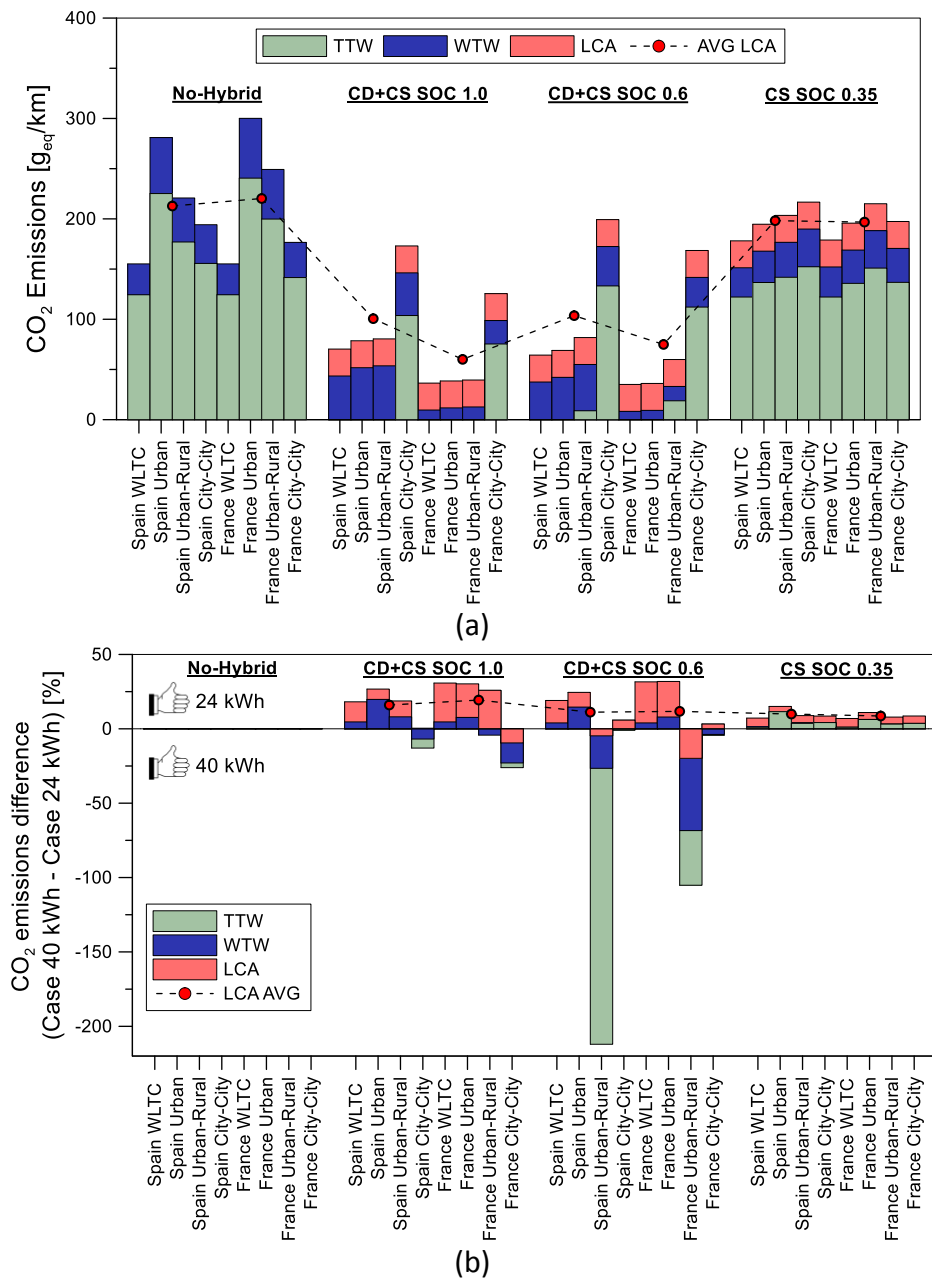




Figure 16 – CO<sub>2</sub> emissions by type (TTW, WTW and LCA) by cycle and country for the hatchback with battery size optimum for energy consumption (a) and the difference against the optimum for minimum environmental impact (b).

The same analysis is applied for the SUV with battery sizes of 48 kWh and 24 kWh. For the brevity of the manuscript, the average results of the three type of driving cycles for each operative mode are summarized in Table 8. As was seen in the optimization analysis, the SUV benefits of using the PHEV 2S-ROPE powertrain are larger in charge depleting mode. However, the charge depleting mode shows higher energy consumption and tank-to-wheel CO<sub>2</sub> emissions, due to non-urban driving cycles. The diesel no-hybrid powertrain has higher efficiency when the battery is depleted in the PHEV. Other disadvantage of the SUV with respect to the hatchback is the replacement of the battery due to the high required vehicle life. Therefore, the LCA values are much higher than in the hatchback case. Overall, the SUV shows good behavior with operation with the initial state of charge at 100% or 60%. With the battery total discharge the no-hybrid shows better results.

Table 8 – Summary of real driving cycles average results for SUV.

Vehicle Platform	Case	Battery Energy [kWh]	Country	Vehicle Mode	Energy consump [kWh/100km]	TTW [g/km]	WTW [g/km]	LCA [g/km]	
SUV	Baseline	-	Spain	No-Hybrid	58.4	156.9		185	
			France	No-Hybrid	59.0	158.5		187	
	Opt Energy	48	Spain	CD+CS 1.0	30.4	30.8	87.6	151.9	
				CD+CS 0.6	30.8	41.6	91.4	155.7	
				CS 0.35	63.0	166.2	206.0	270.2	
				CD+CS 1.0	28.3	22.0	39.1	103.3	
			France	CD+CS 0.6	29.8	38.4	56.7	121.0	
				CS 0.35	62.0	162.8	203.0	267.3	
				CD+CS 1.0	29.9	35.8	87.8	119.9	
				CD+CS 0.6	31.7	50.3	95.8	127.9	
	Opt CO <sub>2</sub>	24	Spain	CS 0.35	58.2	158.2	190.0	222.2	
				CD+CS 1.0	28.5	30.2	47.6	79.7	
				France	CD+CS 0.6	31.1	48.9	68.2	100.4
					CS 0.35	58.0	151.8	189.5	221.6

#### 4. Conclusions

The study shows a novel internal combustion engine technology operating with

opposed piston based on rod-less innovative kinematics in a PHEV series architecture. The potential of this engine is based on its compactness, and preliminary competitive figures in terms of power density and fuel consumption. The novel ICE has been analyzed to be used in a series plug-in hybrid architecture with a OD-vehicle model. Homologation and real driving cycles are used to analyze the impact of the country that is used and the driving modes. Two vehicle platforms (hatchback and SUV) are used as the main representative passenger vehicles in Europe. The main findings of the work are listed as follows:

- The optimum battery size for minimize the energy consumption is 40 kWh for the hatchback and 48 kWh for the SUV.
- Considering the effect of WTW and LCA CO<sub>2</sub> emissions, it was found 24 kWh for both vehicle platforms the best case.
- The test in real driving conditions with 100% of battery charge shows that in urban condition is possible to reduce up to 80% of the energy consumption and more than 75% the CO<sub>2</sub> emissions in life cycle terms.
- The charge sustaining mode shows lower emissions than the no-hybrid, but far from the European CO<sub>2</sub> targets.
- The SUV shows lower benefits than the hatchback due to the higher vehicle weight and aerodynamic resistance.
- For the SUV, the use of a diesel engine in the baseline case makes that the benefits found in the hatchback are strongly reduced.
- The SUV results shows that an initial battery charge above 60% is necessary to have lower greenhouse emissions than the no-hybrid diesel version.
- 24 kWh battery size is the optimum selection to minimize energy consumption and CO<sub>2</sub> emissions based in the real driving cycle analysis for both platforms.

The PHEV with the 2S-ROPE shows great improvements to reduce the energy consumption and emissions. In the next future, user effect as split between cycles along the vehicle use and charging frequency needs to be contemplated. In addition, an ICE version with higher brake power in order to fulfill the SUV requirements under high cargo mass as trailer is needed to be investigated.

### **Acknowledgments**

This work has been partially supported by “Conselleria de Innovación, Universidades, Ciencia y Sociedad Digital de la Generalitat Valenciana” through grant number GV/2020/017. The authors acknowledge FEDER and Spanish Ministerio de Economía y Competitividad for partially supporting this research through TRANCO project (TRA2017-87694-R). The authors want to thank INNengine for providing the engine and the help in the experimental campaign. Lastly, acknowledge to Gamma Technologies for the numerical simulation support and provide the GT-RealDrive licenses.

### **References**

- [1] Thiel C, Nijs W, Simoes S, Schmidt J, van Zyl A, Schmid E. The impact of the EU car CO<sub>2</sub> regulation on the energy system and the role of electro-mobility to achieve transport decarbonisation. *Energy Policy* 2016;96:153–66. doi:10.1016/j.enpol.2016.05.043.

- [2] Cox B, Bauer C, Mendoza Beltran A, van Vuuren DP, Mutel CL. Life cycle environmental and cost comparison of current and future passenger cars under different energy scenarios. *Appl Energy* 2020;269:115021. doi:10.1016/j.apenergy.2020.115021.
- [3] Pareschi G, Küng L, Georges G, Boulouchos K. Are travel surveys a good basis for EV models? Validation of simulated charging profiles against empirical data. *Appl Energy* 2020;275:115318. doi:10.1016/j.apenergy.2020.115318.
- [4] Lane B, Shaffer B, Samuelsen S. A comparison of alternative vehicle fueling infrastructure scenarios. *Appl Energy* 2020;259:114128. doi:10.1016/j.apenergy.2019.114128.
- [5] Conway G, Chambon P. Opportunities for Electrified Internal Combustion Engines 2020:1–11. doi:10.4271/2020-01-0281.Abstract.
- [6] Anselma PG, Biswas A, Belingardi G, Emadi A. Rapid assessment of the fuel economy capability of parallel and series-parallel hybrid electric vehicles. *Appl Energy* 2020;275:115319. doi:10.1016/j.apenergy.2020.115319.
- [7] Luján JM, García A, Monsalve-Serrano J, Martínez-Boggio S. Effectiveness of hybrid powertrains to reduce the fuel consumption and NOx emissions of a Euro 6d-temp diesel engine under real-life driving conditions. *Energy Convers Manag* 2019;199:111987. doi:10.1016/j.enconman.2019.111987.
- [8] Guille des Buttes A, Jeanneret B, Kéromnès A, Le Moyne L, Pélissier S. Energy management strategy to reduce pollutant emissions during the catalyst light-off of parallel hybrid vehicles. *Appl Energy* 2020;266:114866. doi:10.1016/j.apenergy.2020.114866.
- [9] Winklhofer E, Hirsch A, Philipp H, Triffterer M, Berglez M. Powertrain Calibration Techniques. *SAE Tech. Pap. Ser.*, vol. 1, 2019. doi:10.4271/2019-24-0196.
- [10] García A, Monsalve-Serrano J, Martínez-Boggio S, Wittek K. Potential of hybrid powertrains in a variable compression ratio downsized turbocharged VVA Spark Ignition engine. *Energy* 2020;195:117039. doi:10.1016/j.energy.2020.117039.
- [11] Zanelli A, Millo F, Barbolini M, Neri L. Assessment through Numerical Simulation of the Impact of a 48 V Electric Supercharger on Performance and CO<sub>2</sub> Emissions of a Gasoline Passenger Car. *SAE Tech Pap Ser* 2019;1:1–13. doi:10.4271/2019-01-1284.
- [12] Küfeoğlu S, Khah Kok Hong D. Emissions performance of electric vehicles: A case study from the United Kingdom. *Appl Energy* 2020;260. doi:10.1016/j.apenergy.2019.114241.
- [13] Xu X, Aziz HMA, Liu H, Rodgers MO, Guensler R. A scalable energy modeling framework for electric vehicles in regional transportation networks. *Appl Energy* 2020;269:115095. doi:10.1016/j.apenergy.2020.115095.
- [14] Solouk A, Tripp J, Shakiba-Herfeh M, Shahbakhti M. Fuel consumption assessment of a multi-mode low temperature combustion engine as range extender for an electric vehicle. *Energy Convers Manag* 2017;148:1478–96.

doi:10.1016/j.enconman.2017.06.090.

- [15] Borghi M, Mattarelli E, Muscoloni J, Rinaldini CA, Savioli T, Zardin B. Design and experimental development of a compact and efficient range extender engine. *Appl Energy* 2017;202:507–26. doi:10.1016/j.apenergy.2017.05.126.
- [16] Xie S, Qi S, Lang K, Tang X, Lin X. Coordinated management of connected plug-in hybrid electric buses for energy saving, inter-vehicle safety, and battery health. *Appl Energy* 2020;268:115028. doi:10.1016/j.apenergy.2020.115028.
- [17] Ribau J, Silva C, Brito FP, Martins J. Analysis of four-stroke, Wankel, and microturbine based range extenders for electric vehicles. *Energy Convers Manag* 2012;58:120–33. doi:10.1016/J.ENCONMAN.2012.01.011.
- [18] Karvountzis-Kontakiotis A, Andwari AM, Pesyridis A, Russo S, Tuccillo R, Esfahanian V. Application of Micro Gas Turbine in Range-Extended Electric Vehicles. *Energy* 2018;147:351–61. doi:10.1016/J.ENERGY.2018.01.051.
- [19] Kéromnès A, Delaporte B, Schmitz G, Le Moyne L. Development and validation of a 5 stroke engine for range extenders application. *Energy Convers Manag* 2014;82:259–67. doi:10.1016/j.enconman.2014.03.025.
- [20] Bassett M, Hall J, Warth M. Development of a dedicated range extender unit and demonstration vehicle. 2013 World Electr Veh Symp Exhib EVS 2014 2014:1–11. doi:10.1109/EVS.2013.6914833.
- [21] Fan L, Zhang Y, Dou H, Zou R. Design of an integrated energy management strategy for a plug-in hybrid electric bus. *J Power Sources* 2020;448:227391. doi:10.1016/j.jpowsour.2019.227391.
- [22] Requena G. European Patent Office. EP 3 066 312 B1, n.d.
- [23] Serrano, J.R., H. Climent, J.J. López AGV, Garrido J, Requena MJLB and FJCA. DIRECT INJECTION 2-STROKE ENGINES INTERNATIONAL WORKSHOP & CONFERENCE. DIRECT Inject. 2-STROKE ENGINES Int. Work. Conf., Paris: 2020.
- [24] García A, Carlucci P, Monsalve-Serrano J, Valletta A, Martínez-Boggio S. Energy management strategies comparison for a parallel full hybrid electric vehicle using Reactivity Controlled Compression Ignition combustion. *Appl Energy* 2020;272:115191. doi:10.1016/j.apenergy.2020.115191.
- [25] Xu G, Li W, Xu K, Song Z. An intelligent regenerative braking strategy for electric vehicles. *Energies* 2011;4:1461–77. doi:10.3390/en4091461.
- [26] INNengine. INNEngine PHEV concept n.d. <http://innengine.com/> (accessed October 1, 2020).
- [27] Petersheim MD, Brennan SN. Scaling of hybrid-electric vehicle powertrain components for Hardware-in-the-loop simulation. *Mechatronics* 2009;19:1078–90. doi:10.1016/j.mechatronics.2009.08.001.
- [28] Münzel C, Plötz P, Sprei F, Gnann T. How large is the effect of financial incentives on electric vehicle sales? – A global review and European analysis. *Energy Econ* 2019;84:104493. doi:10.1016/j.eneco.2019.104493.

- [29] Nissan. Nissan Vehicles Specifications n.d. <https://www.nissan.es/> (accessed October 1, 2020).
- [30] He Y, Wang C, Zhou Q, Li J, Makridis M, Williams H, et al. Multiobjective component sizing of a hybrid ethanol-electric vehicle propulsion system. *Appl Energy* 2020;266. doi:10.1016/j.apenergy.2020.114843.
- [31] Hao X, Lin Z, Wang H, Ou S, Ouyang M. Range cost-effectiveness of plug-in electric vehicle for heterogeneous consumers: An expanded total ownership cost approach. *Appl Energy* 2020;275:115394. doi:10.1016/j.apenergy.2020.115394.
- [32] CONCAWE; EUCAR; JRC. EU renewable energy targets in 2020: Revised analysis of scenarios for transport fuels. 2014. doi:10.2790/1725.
- [33] European Commission. Regulation (EU) 2019/631 of the European Parliament and of the Council of 17 April 2019 setting CO<sub>2</sub> emission performance standards for new passenger cars and for new light commercial vehicles, and repealing Regulations (EC) No 443/2009 and (EU) No 510/2011. *Off J Eur Union* 2019;62:80.
- [34] Agency IE. Electricity information: Overview (2020 edition) 2020.
- [35] Qiao Q, Zhao F, Liu Z, Jiang S, Hao H. Comparative Study on Life Cycle CO<sub>2</sub> Emissions from the Production of Electric and Conventional Vehicles in China. *Energy Procedia* 2017;105:3584–95. doi:10.1016/j.egypro.2017.03.827.
- [36] Ellingsen LA-W, Singh B, Strømman AH. The size and range effect: lifecycle greenhouse gas emissions of electric vehicles. *Environ Res Lett* 2016;11:054010. doi:10.1088/1748-9326/11/5/054010.
- [37] Dun C, Horton G, Kollamthodi S. Report for European Commission: Improvements To the Definition of Lifetime Mileage of Light Duty Vehicles. 2015.
- [38] Henschel J, Horsthemke F, Stenzel YP, Evertz M, Girod S, Lürenbaum C, et al. Lithium ion battery electrolyte degradation of field-tested electric vehicle battery cells – A comprehensive analytical study. *J Power Sources* 2020;447. doi:10.1016/j.jpowsour.2019.227370.
- [39] Abdul-Manan AFN, Won HW, Li Y, Sarathy SM, Xie X, Amer AA. Bridging the gap in a resource and climate-constrained world with advanced gasoline compression-ignition hybrids. *Appl Energy* 2020;267:114936. doi:10.1016/j.apenergy.2020.114936.
- [40] Graham-Rowe E, Gardner B, Abraham C, Skippon S, Dittmar H, Hutchins R, et al. Mainstream consumers driving plug-in battery-electric and plug-in hybrid electric cars: A qualitative analysis of responses and evaluations. *Transp Res Part A Policy Pract* 2012;46:140–53. doi:10.1016/j.tra.2011.09.008.

## Abbreviations

2S-ROPE	2-stroke rodless opposed piston engine	OEM	Original equipment manufacturer
ATS	Aftertreatment systems	PFI	Port fuel injection
BEV	Battery electric vehicles	PHEV	Plug in electric vehicle
BSFC	Brake specific fuel consumption	rpm	Revolution per minute
BTE	Brake thermal efficiency	SI	Spark Ignition
CD	Charge depleting	SOC	State of the charge of the battery
CI	Compression Ignition	SUV	Sport utility vehicle
CR	Compression ratio	TTW	tank-to-wheel
CS	Charge sustaining	UF	Utility factor
GDI	Gasoline Direct Injection	VCR	Variable compression ratio
EM	Electric motor	VPT	Variable port timing
EU	European Union	WLTC	Worldwide Harmonized Light Vehicles Cycle
FHEV	Full hybrid vehicle	WLTP	Worldwide Harmonized Light Test Procedure
HEV	Hybrid electric vehicle	WTT	Well-to-tank
ICE	Internal combustion engine	WTW	Well-to-wheel
LCA	life-cycle analysis	xHEV	Refers to several hybrid electric vehicles
MHEV	Mild hybrid electric vehicle	NHV	Noise, vibration, and harshness

## Appendix A

Table A1 shows the main characteristics of the A123 pouch cell used in this work to assemble the battery pack. A 20% extra weight is added to the cell weight to contemplate case, electric and cooling system. The cells are arrangement in 121 series cells (400 nominal pack voltage). The number of parallel cells determines the final pack energy and power.

Table A1 – A123 20Ah/3.3 V pouch cell specifications.

Cell Type	Pouch cell
Cell dimensions [mm]	7.25x160x227
Cell weight [g]	496
Battery package extra weight [%]	20
Energy content [Wh]	66
Nominal voltage [V]	3.3
Nominal capacity [Ah]	20 Ah
Specific power [W/kg]	2400
Specific energy [Wh/L]	131
Voltage range [V]	2.0 to 3.6
Maximum charge current [A]	100
Maximum discharge current [A]	200
Operating Temperature range [°C]	-40 to 65
Cycle life to 80% beginning of life capacity [cycles]	3000

## Appendix B

Figure B1 shows the baseline engine maps used to model the ICE fuel consumption for the hatchback and SUV no-hybrid powertrains. The diesel Euro 6-dtemp engine with 1.6L and turbocharger allows to achieve 215 g/kWh (BTE of 39.4%). The gasoline 1.0L turbo engine achieves 240 g/kWh (35.6%) similar to the 2S-ROPE engine.

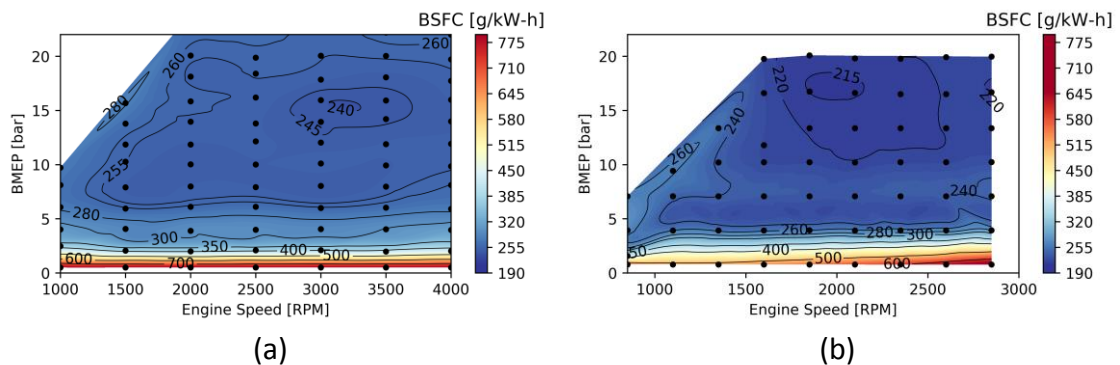


Figure B1 – BSFC maps for the gasoline DISI 1.0 L turbo (a) and diesel DICI 1.6 L engine (b)

## Appendix C

The 60 driving cycles in Spain and France are depicted in Figure C1 to Figure C6. Vehicle speed against time is presented with the marks of the homologation real driving emissions (RDE) speed limits. In this work, the real driving cycles not consider this homologation limits and the time and altitude specified by the WLTP. On the contrary, the objective is to evaluate under real conditions that a random driver can be exposed in the road.



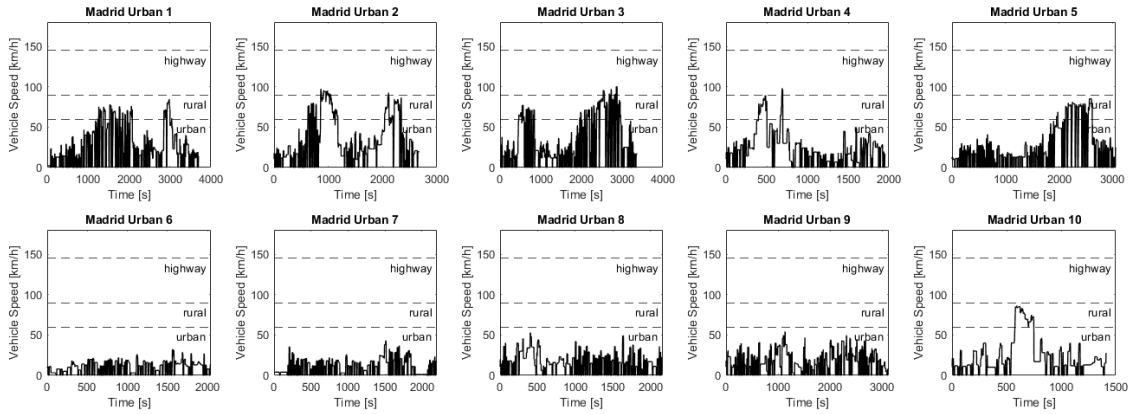


Figure C1 – Spain ten urban driving cycles obtained in Madrid city center with GT-Real Drive tool.

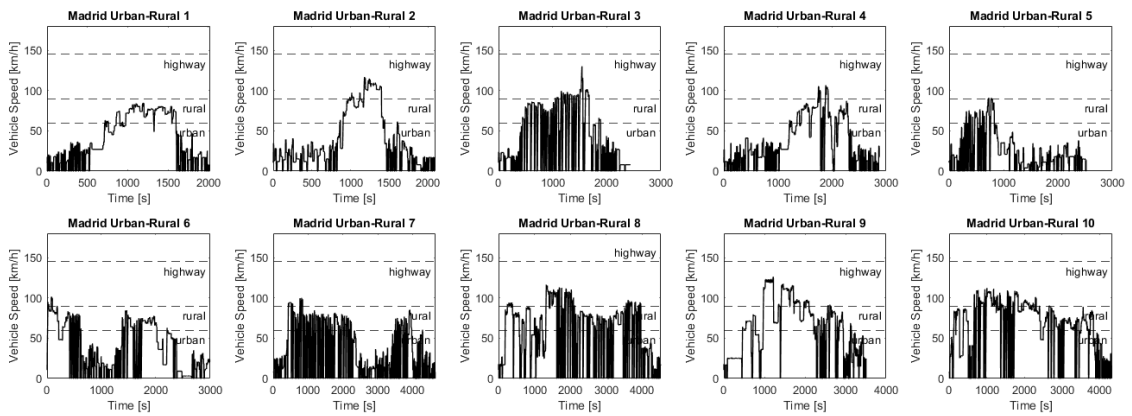


Figure C2 – Spain ten urban-rural driving cycles obtained from Madrid city center to a neighbor town with GT-Real Drive tool.

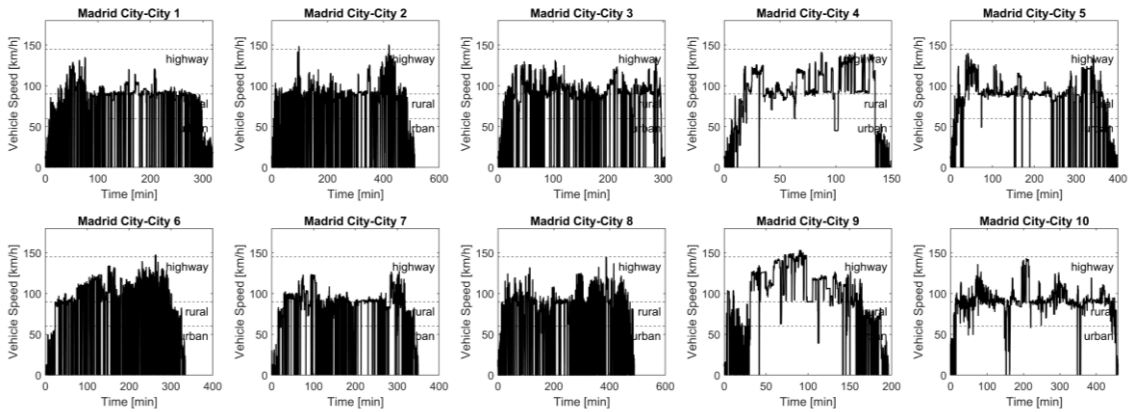


Figure C3 – Spain ten city-city driving cycles obtained from Madrid city center to Valencia, Barcelona, Bilbao, Salamanca, Sevilla, Badajoz, Granada, Vigo, Albacete and Girona with GT-Real Drive tool.

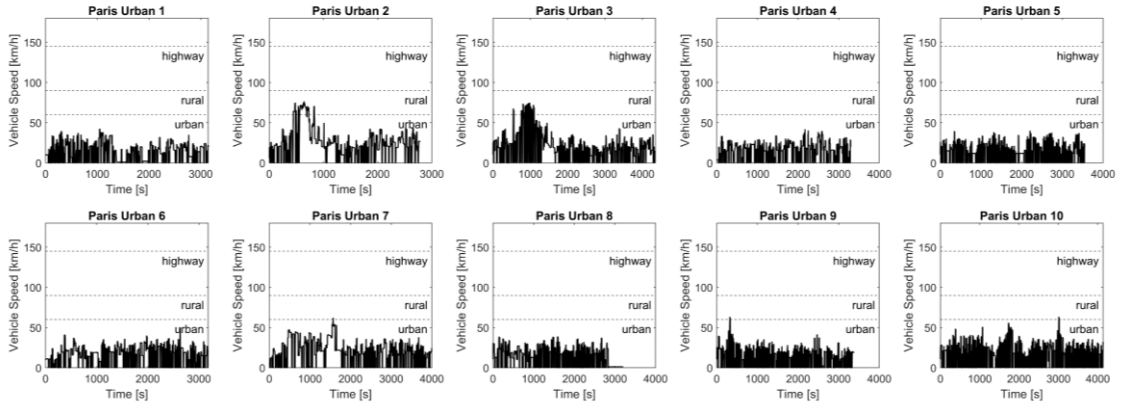


Figure C4 – France ten urban driving cycles obtained in Paris city center with GT-Real Drive tool.

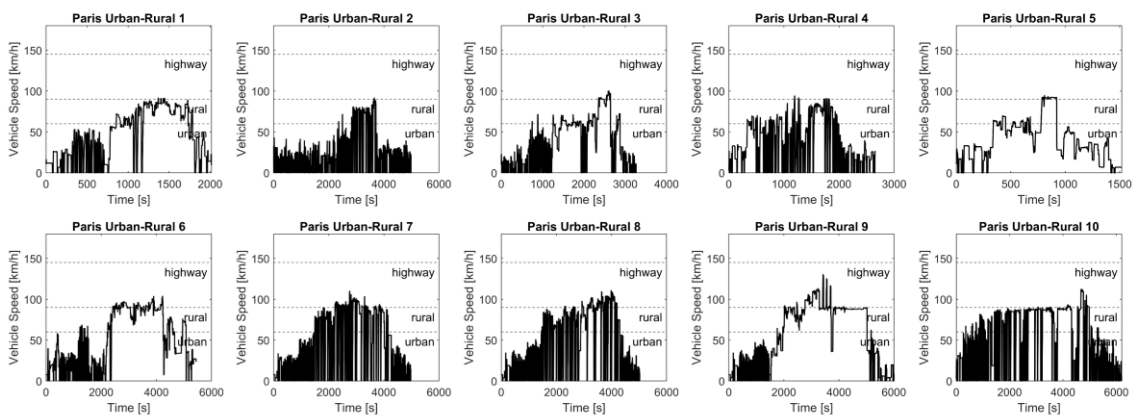


Figure C5 – France ten urban-rural driving cycles obtained from Paris city center to a neighbor town with GT-Real Drive tool.

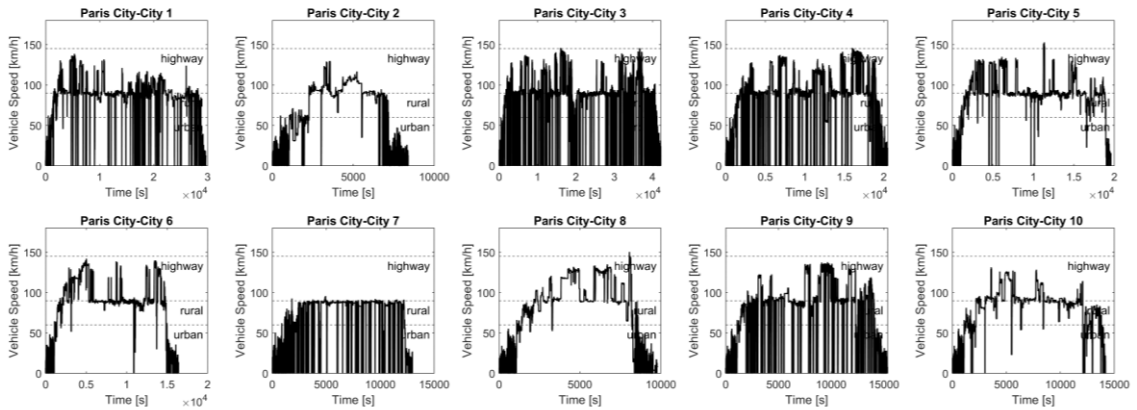


Figure C6 – France ten city-city driving cycles obtained from Paris city center to Toulouse, Rouen, Monaco, Lyon, La Rochelle, Nantes, Lille, Le Mans, Dijon and Saint Lo with GT-Real Drive tool.

## Appendix D

Figure D1 shows the performance analysis when four passenger and the standard cargo mass is applied in the vehicle. In addition, Figure D2 shows the performance curves for the SUV with a trailer (1000 kg).

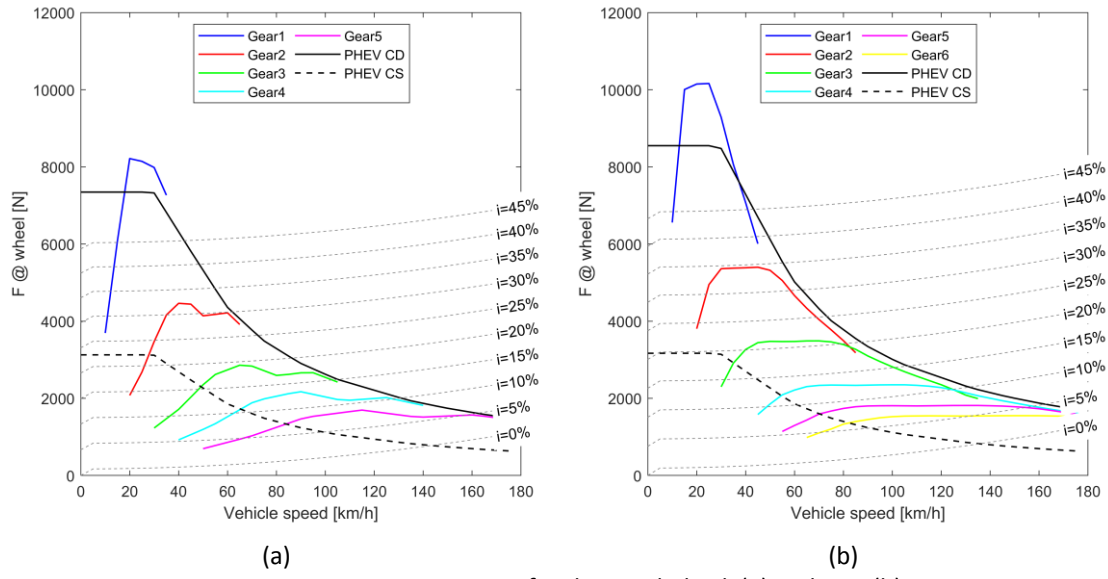


Figure D1 – Four Passengers for the Hatchback (a) and SUV (b)

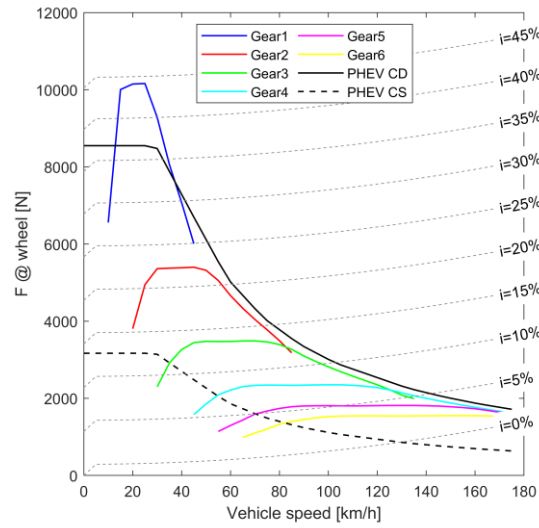


Figure D2 – Four passengers and trailer for the SUV